Effects of building layouts and envelope features on wind flow and pollutant exposure in height-asymmetric street canyons

Dongjin Cui[1], Xingdi Li[1], Jianlin Liu[2]*, Cheuk Ming Mak[3], Kenny Kwok[4]

[1]*School of Architecture and Urban Planning, Shenzhen University, China*
[2]*College of Environmental Science and Engineering, Donghua University, Shanghai, China*
[3]*Department of Building Services Engineering, The Hong Kong Polytechnic University, Hong Kong*
[4]*School of Civil Engineering, The University of Sydney, Australia*
*Corresponding email: jian-lin.liu@connect.polyu.hk

Abstract

The influences of building layouts on pollutant dispersion within urban street canyons have been widely studied, while they are rarely considering with envelope features. Different envelope features, such as wing wall, balcony and overhang, have not yet been quantitatively assessed their effects on the wind flow patterns around street canyons to a certain degree. Adopting the evaluation indicators of personal intake fraction and daily pollutant exposure, this study aims to investigate the potential influences of building layouts and envelope features that happen to the pollutant exposure risks for pedestrians and near-road residents via computational fluid dynamics (CFD). Turbulence modelling approach and numerical methods are validated by reported experiments in literature. Asymmetric street canyons with an aspect ratio of 2 and two typical building layouts, namely step-up and step-down notch configurations, are further investigated to test their effects. Results indicate that the step-down configuration provide in worse situations for wind environments and pollutant dispersion, compared to the symmetric and step-up configurations. More specifically, the presence of overhangs has the greatest impact

on the *P_IF* change ratio, followed by balconies. The largest *P_IF* change ratio occurs to the fifth floor of the upstream building, when overhangs are applied to the step-down street canyon. The aforementioned findings are helpful to understand the influences of building layouts together with envelope features on the wind environment as well as pollutant exposure risks experienced by pedestrians and near-road residents.

Keywords: *envelope features; building layouts; CFD simulation; pollutant exposure; pedestrian-level wind (PLW)*

1. Introduction

With the global urbanization mushrooming continuously, traffic emission has been one of the main contributors to urban air pollution, which can do serious harm to public health [1,2]. Additionally, the presence of windows, building cracks and ventilation systems allows vehicular exhaust to enter the indoor space [3]. Consequently, apart from pedestrians, citizens whose houses are adjacent to traffic roads are the best possibilities to suffer from vehicular pollutants.

According to existing investigations, there are many factors affecting urban ventilation, including building height variations (uneven urban layouts) [4], building packing density [5], lift-up designs [6-8], street shapes [9] and ambient wind directions [10,11]. So far, a series of studies have been performed on urban street canyons. Commonly-used in urban areas, the influences of asymmetrical street configurations on pedestrian environments cannot be ignored [12]. Li et al. [13] undertook researches on the microclimate inside step-up and step-down canyons, with the lower building's height changing. They finally concluded that the pollution situation would get worse in the step-up canyon when the upwind building got taller. However, when the downwind building became taller in the step-down canyon, the pollutant

concentration only increases at the smaller wind velocity. To further understand this issue, Park et al. [14] defined the building-length ratio as the ratio of building length to the canyon width. They pointed out that a slight reduction would happen to the reverse flow, updraft and streamwise flow within the step-up canyon, when the building-length ratio increased. According to these previous studies, we can easily find out that most researchers mainly focused on the aspect ratios, building-length ratios, building height variations and so on. But the combination of building layouts and envelope features haven't received much attention yet.

As an indispensable element shaping metropolis, the envelope feature can affect the natural ventilation [15] to a nonnegligible degree. Researches conducted by Ai and Mak [16] demonstrated that the single-sided ventilation inside the target building could benefit from horizontal envelope features, which were set at the center of windows. Ghadikolaei et al. [17] discovered that the introduction of wing walls was conducive to enhancing indoor ventilation, as long as the wing walls acquired appropriate angles and sizes. Obviously, the influences of different envelope features on near-wall airflow have already received a great deal of attentions. However, when it comes to the correlation between the introduction of envelope features and the wind flow patterns inside the street canyon, it is still not fully understood.

Apart from the wind flow pattern, the pollutant dispersion in urban areas has also been discussed in previous studies [5,9]. Nevertheless, it is not enough for in-depth researches on the risks of public exposure to traffic emissions, which hasn't acquired necessary recognition. Adopting high-resolution 2D CFD simulations, we mainly devote ourselves to studying the wind flow patterns inside street canyons as well as pedestrian-level and near-road resident-level pollutant exposure risks. Based on the pollutant concentrations at pedestrian-level and centers of building openings, the values of intake fraction (*IF)*, personal intake fraction (*P_IF*), and daily pollutant exposure are calculated. This method has also been applied to previous literatures [18]. This paper pursues two main goals concerning the combination of asymmetric

configurations and three common envelope features. The asymmetric configurations include step-up and step-down building layouts, and the envelope features consist of balconies, overhangs and wing walls. On the one hand, we thoroughly investigated how this combination affects the airflow patterns and pollutant distributions within street canyons of interest. On the other hand, we also undertook researches on pedestrians' and near-road residents' exposure risks, which achieved quantitative evaluations. The construction of healthy and sustainable cities can take advantage of these efforts.

The remaining sections of this article follow the orders outlined below: Section 2 introduces the research methods adopted in this paper. Section 3 discusses the simulation results. Section 4 summarizes the whole article as well as points out the limitations of current studies. And section 5 presents the limitations of our current work as well as the possible enhancement in the future.

2. Research methods

2.1 Description of computational geometry

In this article, three different kinds of building layouts are considered. **Fig. 1** shows the computational domains of two-dimensional (2D) full-scale street canyons studied in this article, including the symmetric canyon, the step-up canyon and the step-down canyon. For the symmetric canyon, building heights are invariable. The corresponding ratio of the upwind building height to the downwind building height is equal to 1, 2 and 0.5, respectively. As illustrated by **Fig. 1**, this thesis adopted the computational domain of two-dimensional (2D) full-scale street canyon. According to previous studies, there exists two different approaches to coping with the incident wind coming from the inlet of the computational domain. On the one hand, a series of researches applied specific settings of the roughness height K_S and the roughness constant C_S to the domain's upstream and downstream bottom [19]. This option is

for acquiring the atmospheric boundary layer (*ABL*), which is homogeneous in the horizontal direction. On the other hand, researchers also can set a certain number of building models at the upstream and downstream areas, severally. These building models serve as roughness elements, in favour of forming an urban boundary layer [20,21]. In this paper, we chose the second approach. The computational domain consists of five street canyons, namely the target one, the two canyons located at the upstream area, and another two canyons set at the downstream region (see **Fig. 1**). This arrangement is necessary for the accurate reproduction of urban roughness elements. As for the number of building models which should be set at the upstream region, some existing studies introduced two or three upstream street canyons [18,21]. Consequently, in order to get access to a reasonable boundary, this investigation introduced two street canyons and two building units in the upstream region (see **Fig. 1**).

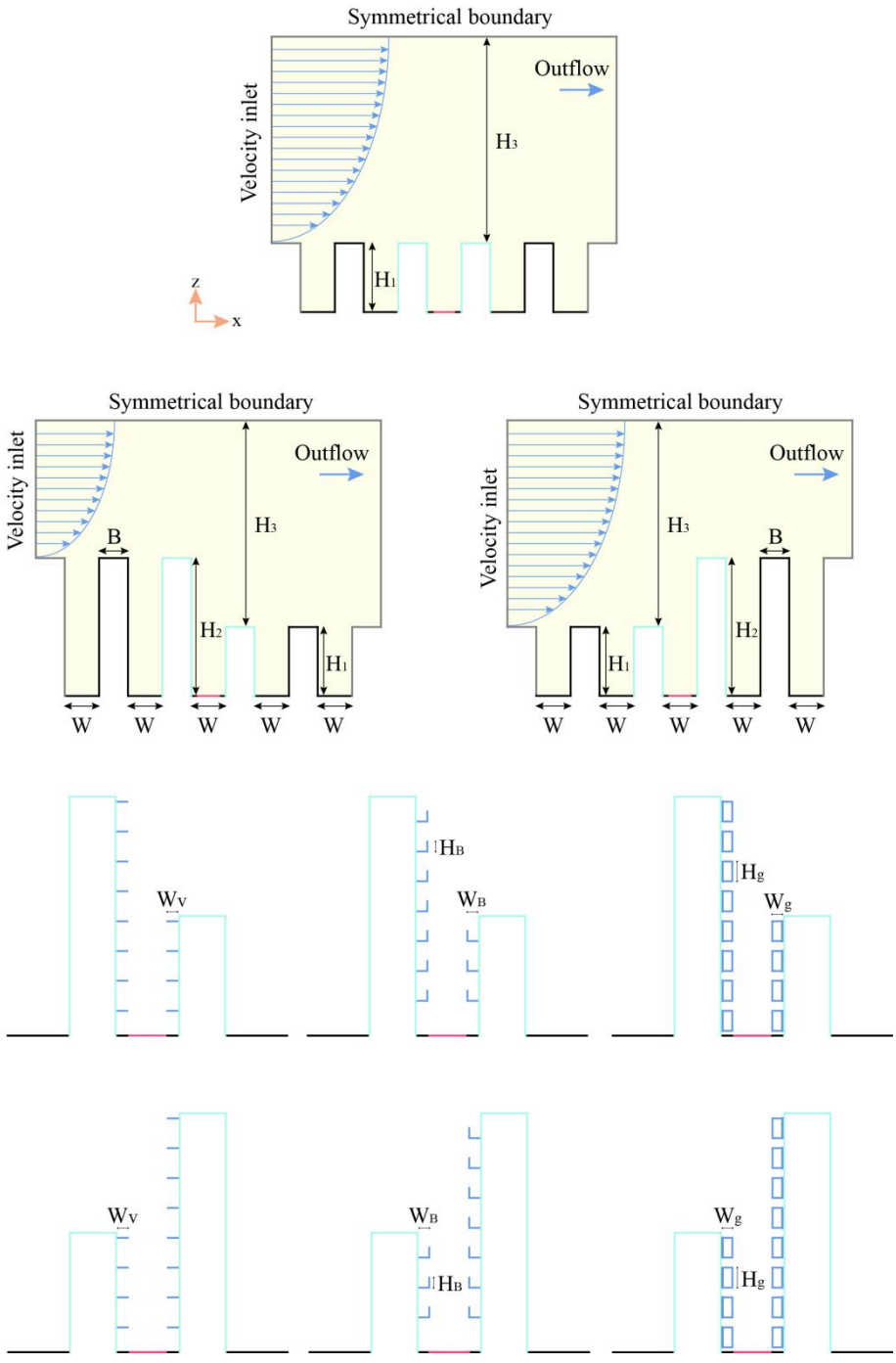

Fig. 1. Sketches of street canyons with flat facades and various envelope features.

In this research, we used the symmetric, step-up and step-down street canyons adopting no envelope features as basic cases (see **Fig. 1**). Based on this, this study revealed how the envelope features affect the wind flow structure and pollutant transmission inside target street canyons.

As illustrated by **Fig. 1**, all the buildings in the symmetric canyon have four floors, and each floor is three meters high with a window located in its center. And all the windows are 2 meters high (H_O) and 4 meters wide (L_O). At the same time, the lower buildings in the asymmetric canyons share the same height (H_1) with those in the symmetric one, which is equal to 12 m. Contrary to this, the heights of all the taller buildings (H_2) are twice the heights of those lower ones, namely 24 m. Additionally, the computational domain roof is 36 and 24 meters above the roofs of the lower and taller buildings, separately. The widths of street canyons (W) are equal to 6m and all the cases simulated in this study applied an aspect ratio (H_1/W) of 2. Focusing on the wind environment in the street canyons, we also set a pedestrian level which is 1.5m above the domain bottom in each case. Furthermore, three common envelope features including overhang, balcony and wing walls (see **Fig. 1**) acquired specific investigations. **Table 1** listed the physical dimensions of all the envelope features, which are cantilevered 1 meter away from the building facades ($W_B = W_V = W_g = 1$ m). In particular, the balconies are 1.5 m high.

Table 1. Summary of physical parameters for deep canyons models.

Envelope features setting	**Case Name**		**Fixed values**
Basic cases (Flat facades)	**NS**	**N (**Symmetric**)**	U_{ref} = 4 m/s
	Nu	**N (**Step-up**)**	
	Nd	**N (**Step-down**)**	
Balcony (H_B = 1.5 m, L_B = 4 m, W_B = 1 m)	**BAu**	**BA (**Step-up**)**	
	BAd	**BA (**Step-down**)**	
Overhang (L_V = 4 m, W_V = 1 m)	**OHu**	**OH (**Step-up**)**	
	OHd	**OH (**Step-down**)**	
Wing walls (H_g = 2 m, W_g = 1 m)	**WAu**	**WA (**Step-up**)**	
	WAd	**WA (**Step-down**)**	

The independence of Reynolds number (*Re*) is necessary for numerical simulations applying reduced-scale models [22]. Considering this independence requirement and cost reductions in computing, the models used in this study were all scaled down at a ratio of 1:15. According to the calculations, the *Re* numbers at the heights of buildings and around the envelope features are near 2.4×10^5 and larger than 1×10^4 averagely, which meets the independence requirement [22]. On the basis of cell numbers, a series of tests were conducted on grid sensitivities for the symmetric case without any envelope features, for purpose of keeping the numerical simulations independent. In the tests, we adopted three kinds of grids including the coarse grid, the medium grid and the fine one, which were all high-resolution ($y^+ < 10.0$) for meshing and resolving the near-wall boundary layer on the whole. And the latter two grids were obtained by resetting the coarse grid applying a factor of 1.5. **Fig. 2** described in detail the information of grid on a vertical bounded surface across the two buildings on both sides of the target street canyon. It's clear that the computational domain consists of only hexahedra (see **Fig. 2**) and the minimum cell size is equal to 0.0006 m, 0.0004m and 0.0027m in the coarse grid, medium grid and fine grid separately. Additionally, for all cases the mesh stretching ratio is always less than 1.08. Hence, the numbers of cells for the symmetric basic case using the coarse, medium and fine grid end up being 1.07 million, 8.71 million and 10.21 million averagely. It's noteworthy that the number of cells in cases adopting envelope features is larger that in cases using flat facades, when the building layout remains the same (see **Fig. 2**). According to the mesh sensitivity test along the center line of the target canyon (see **Fig. 2**), we finally chose the medium grid throughout the study. This is because the mean deviation between the simulation results by the coarse grid and the medium grid is as large as 37.9%, while the deviation between the medium and fine grids is only 8.0%. It's obvious that the medium grid can achieve a good balance between saving computing cost and ensuring sufficient simulation accuracy. Other

cases choosing asymmetric layouts shared the same grid settings with the symmetric street canyon.

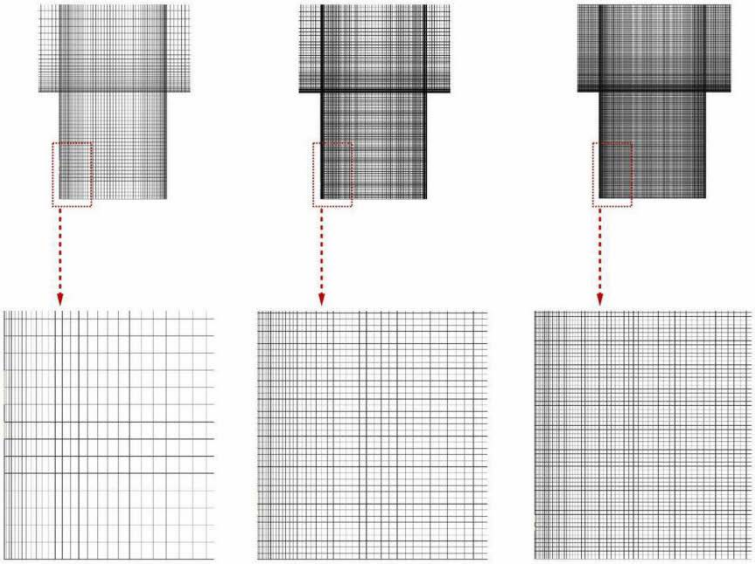

(a)

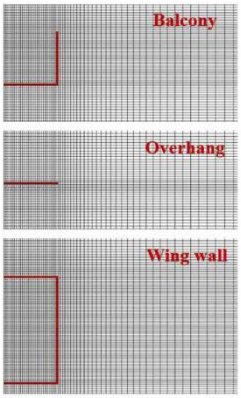

(b)

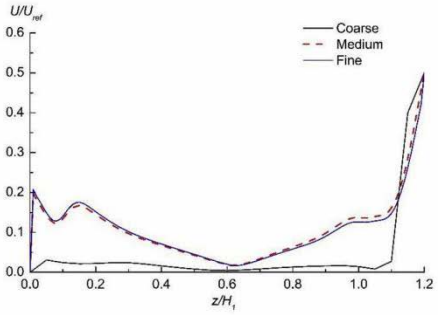

(c)

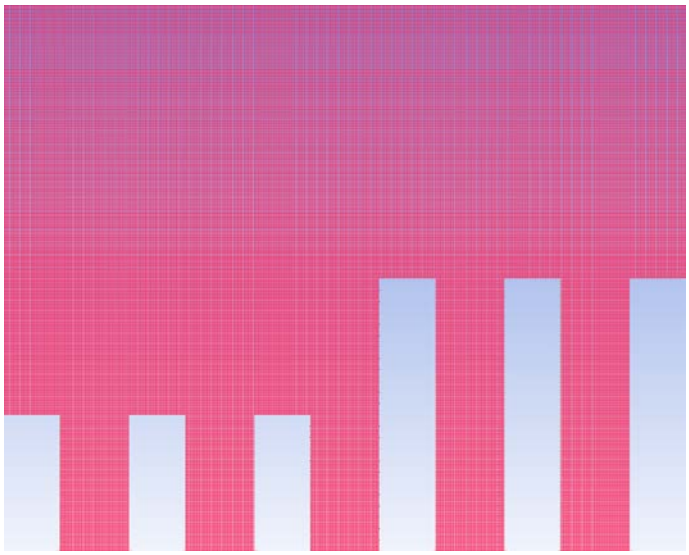

(d)

Fig. 2. (a) Detailed mesh information for all the cases; (b) Mesh around envelop features; (c) Sensitivity test results; and (d) Mesh for case Nu.

2.2 Metrics for pollutant exposure

The intake fraction (*IF*) has been adopted by previous studies concerning traffic emissions, serving as an important index to evaluate the pollutant exposure of populations with different ages in urban micro-environment [18,23]. *IF* describes the average amount of pollutants inhaled per person from the total amount of pollutants emitted. When the traffic source discharges 1 kg of pollutants, 1 mg of which is inhaled by the target population, *IF* is equal to 1 ppm (one per million, 10^{-6}). Additionally, the indicator of daily pollutant exposure can describe the extent, to which the target population is affected by pollutants throughout a day [24]. Quantifying the evaluation of pollutant exposure risks is in favour of assessing various pollutant sources, such as motor vehicles. This paper used both the *IF* and the concept of daily pollutant exposure.

2.2.1 Pollutant intake fraction (*IF*) and personal intake fraction (*P_IF*)

Adopted in series of literatures, the pollutant intake fraction (*IF*) indicates how much the target population has inhaled from the total emissions (e.g., gaseous traffic pollutants). As for an urban region of interest, the value of *IF* can be calculated by Eq. (1):

$$IF = \sum_{i}^{N}\sum_{j}^{M} P_i B_{i,j} \Delta t_{i,j} C_j \Big/ q \tag{1}$$

where N indicates that the target population contains a total of N age groups while i represents the ith age group. P_i means the number of people exposed to vehicular emissions in the ith age group. Based on the population census data [25] (**Table. 3**), the value of N was set to 3 in this article. Additionally, M and j are the sum of all the different micro-climate conditions and the jth micro-climate condition separately. This study mainly focused on pedestrians and near-road residents. Consequently, we considered four conditions (M = 4) [26] (**Fig. 2**), including indoor at home (j = 1), other indoor locations (j = 2), outdoor near vehicles (j = 3), and other outdoor locations (j = 4). $B_{i,j}$ and $\Delta t_{i,j}$ denote the average volumetric breathing rate (m^3/s) (**Table. 2**) and the stay time of the ith age group (**Fig. 2**) under the jth micro-climate respectively [25,26]. C_j is the pollutant concentration at a particular location within the street canyon. Finally, q represents the total discharge of the pollutants.

Furthermore, based on the *IF* and the demographic structure, this research adopted the personal intake fraction (*P_IF*). This allowed the population density to keep independent. And the *P_IF* can be defined as below:

$$P\_IF = IF \Big/ \sum_{i}^{N} P_i \tag{2}$$

Table 2. Breathing rate for various age groups under different micro-environments.

Breathing rate Br(m^3/day)	**Indoor at home** (j = 1)	**Other indoor locations** (j = 2)	**Outdoor Near Vehicles** (j = 3)	**Other outdoor locations** (j = 4)
Children (i = 1)	12.5	14	14	18.7
Adults (i = 2)	13.8	15.5	15.5	20.5
Elderly (i = 3)	13.1	14.8	14.8	19.5

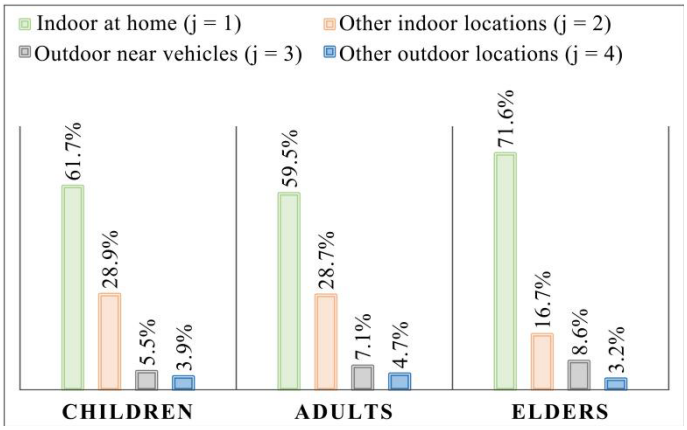

Fig. 2. Time activity patterns for different age groups and micro-environments.

Table 3. Demographic structure in Shenzhen, China.

Age Groups	Children (<14)	Adults (15-64)	Elders (>65)
Demographic Percentage	13.40%	83.20%	3.40%

2.2.2 Daily pollutant exposure indicator

To describe quantitatively the extent of target populations' exposure to traffic emissions throughout the day, the daily pollutant exposure is defined as follows:

$$E_d = \sum_{j}^{M} E_{d,j} = \sum_{j}^{M} \sum_{i}^{N} C_j t_{i,j} \quad (3)$$

where, the definitions of i, N, j, M, C_j and $t_{i,j}$ are exactly the same as those in Eq. (1), which are described clearly in **Fig. 2, Table.2** and **Table. 3**.

2.3 Turbulence modeling validation

2.3.1 Validation for wind flow

A water tunnel ($L_T \times W_T \times H_T$: 10 m × 0.3 m × 0.5 m) experiment was performed by Li et al. [27], measuring the wind flow field within the target street canyon. A series of researches have used this experiment to verify turbulence models [28,29]. Consisting of eight and ten selfsame architectural models averagely, two different kinds of street canyons whose aspect ratios ($AR = H_B/W_S$) were equal to 1.0 and 2.0 separately were applied. All the building models shared a same height and it was unchangeable, equal to 0.1 m (H_B = 0.1 m). Meanwhile, the depth of the water was unchangeable too, equal to 0.4 m in the two groups of experiments. The direction of the approaching water flow was perpendicular to the investigated street canyons (**Fig. 3**b). According to the reference speed of water (U_{ref} = 1.8 m/s), the Reynolds number at the height of building models and 0.3 m were both equal to 12,000. There didn't exist any roughness elements in those experiments. Additionally, two horizontal and three vertical lines were set on the vertical surface located at the center of the target street canyon (y = 0) (**Fig. 3**a). Along these

lines, the researchers adopted a two-colour laser Doppler anemometer (LDA) to acquire the velocity components in the vertical and streamwise directions.

The geometry of buildings and the street canyon (see **Fig. 3**a and b) adopted by Li et al. [27] were also applied to the numerical simulations based on CFD. According to the available best guidelines for CFD simulations of urban aerodynamics [30,31], we constructed the computational domain, whose height and lateral length were just the same as those in the water tunnel experiments. There was nothing but a series of structured hexahedral units that formed the computational domain (see **Fig. 3**c). The cases of AR = 1.0 and 2.0 ended up adopting 3,168,000 and 2,880,000 cells averagely, resulting from a test for the grid sensitivity. With the average value of y^+ equal to 5.3, the first units close to the walls and ground is 1.665 mm high, at which the value of y^+ varied from 0 to 15. Due to the relatively high wind velocity, the top corners of the windward sides were the only places where the highest value of y^+ would appear.

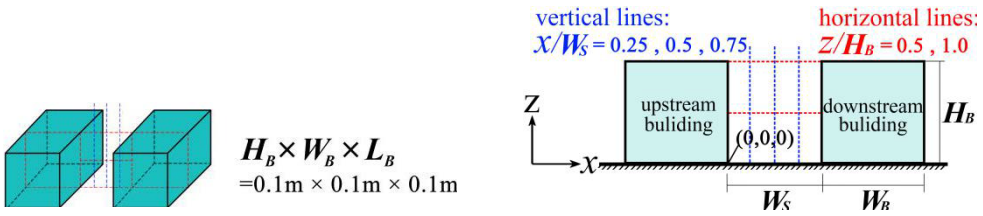

(a)

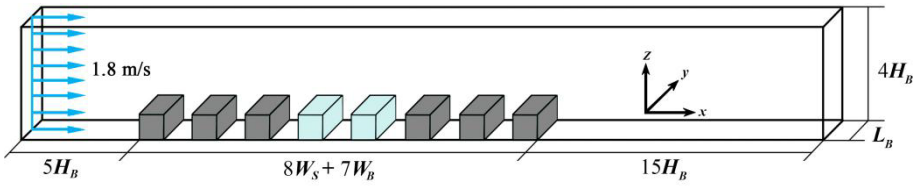

(b)

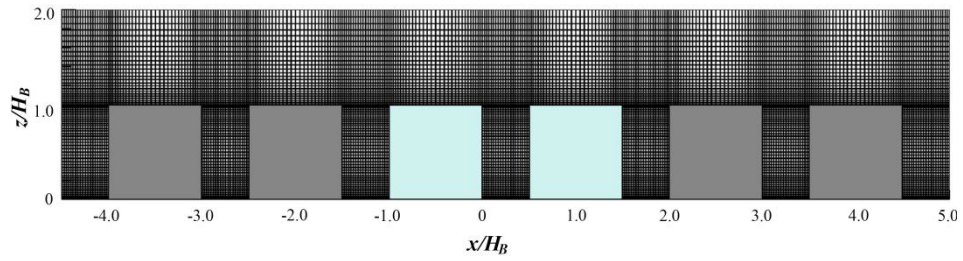

(c)

Fig. 3. (a) Canyon geometry and measurement lines; (b) computational domain; and (c) grid arrangement on vertical center-plane (AR = 2).

As for the computational domain, the wind velocity at the inlet is uniform and equal to that used in those experiments, namely 1.8 m/s. The turbulent intensity and turbulent length scale of the inflow were set as 5% and 0.35 m respectively, on the basis of a sensitivity test of the inflow's turbulent characteristics against the data for the velocity field in the experiments. Additionally, pressure outlet together with zero static pressure were applied to the domain outlet. In terms of the domain's top and the lateral sides, we adopted zero normal velocity and zero normal gradients of all variables. Finally, non-slip walls were defined for the ground of the domain as well as the surfaces of buildings.

In this investigation, we have chosen the commercial code ANSYS FLUENT 15.0 as the tool for numerical simulations. The steady-state two-equation Reynolds-Averaged Navier-Stokes (RNAS) model is good at simulating the airflow inside and around buildings [32]. Hence, it was applied to simulate the flow and turbulent fields in this study. Additionally, the near-wall regions were treated using the two-layer model. For purpose of coupling the pressure and momentum equations, SIMPLEC algorithm was adopted. The discretization of convection and diffusion terms can be attributed to the presence of the second-order schemes. With all the

scaled residuals below 10^{-5} and the averaged wind velocity at representative locations inside the canyon keeping unchangeable after 50 iterations, the convergence was finally acquired.

As shown by **Fig. 4**, we compared the experimental data of the velocity components in x direction with that acquired from numerical simulations. **Fig. 3** has described the locations of those comparison lines clearly. According to the comparison results (see **Fig. 4**), the relative deviation between the numerical data and experimental data keeps below 10% averagely, denoting that these two types of data agree well with each other. Previous literatures [27] also have mentioned this degree of difference between the simulation data and experimental results.

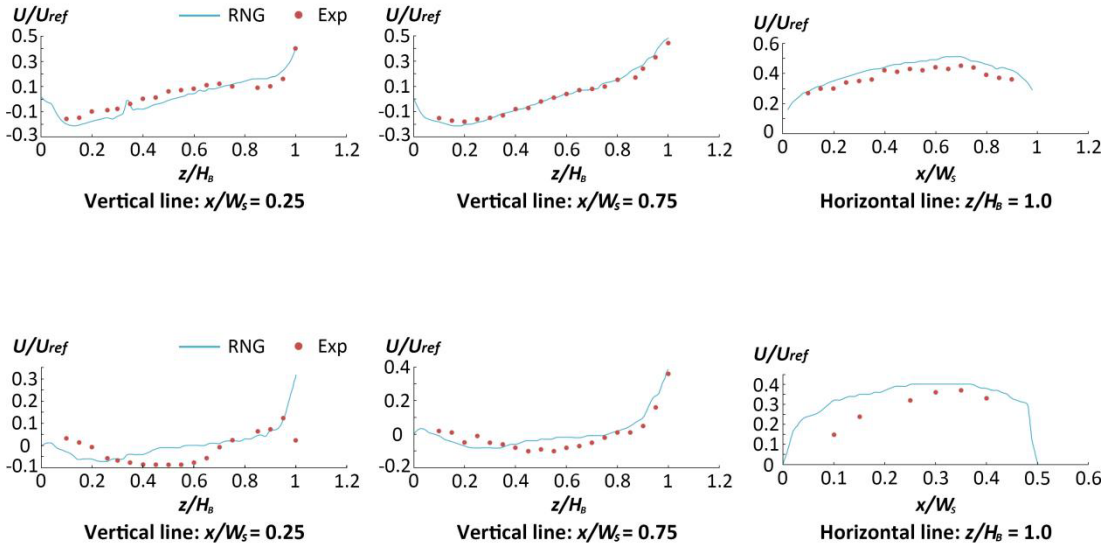

Fig. 4. Velocity components in x and z directions along two horizontal lines and four vertical lines on the vertical center-plane of the target street canyon.

2.3.2 Validation for pollutant transmission

On the basis of the wind tunnel experiments performed by Li and Meroney [33], this study realized the validation for the pollutant transmission. In this experiment, there existed a building model with cubic shape, which was immersed in a neutrally stratified turbulent atmospheric boundary layer. The profile of the approaching wind obeyed a power law whose exponent is

equal to 0.19. Reaching the building model perpendicularly, the incident wind has a velocity of 3.3 m/s at the building height. The pollutant source was located at the center of the building's roof, discharging the mixture of air and helium at a speed of 0.627 m/s. The researchers also measured the concentration of pollutants at various locations behind the building (see **Fig. 5**). The literature by Li and Meroney [33] described this wind tunnel experiment at great length. It's worth noting that the turbulence models and numerical settings mentioned in section 2.3.2 were also applied to the simulations for pollutant transmission. At the same time, we also solved the species transport equation, namely equation (6). This investigation used the non-dimensional concept of concentration ratio, which meant the ratio of the local pollutant concentration (C) to the reference pollutant concentration (C_0) at the pollutant source. Similar to the validation for wind flow, the simulation results were compared to the wind tunnel experiment data (see **Fig. 5**). Overall, the deviations between these two types of data were always below 10% denoting that they agreed well with each other. It is evident that the turbulent models and numerical settings chosen by this study were good enough to simulate the flow field pollutant transmission within target canyons. Consequently, all of them were applied to the remaining parts of this article.

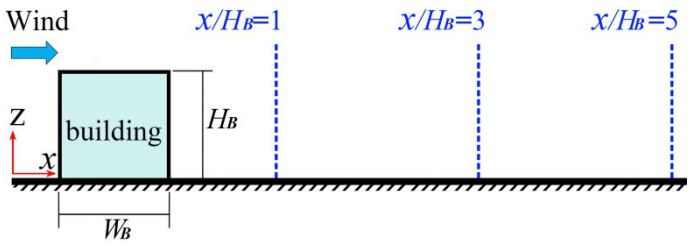

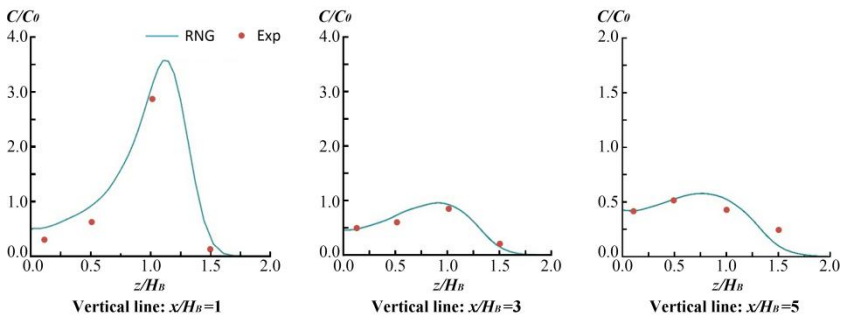

Fig. 5. Validation of CFD simulation results by comparison with wind tunnel data.

2.4 Boundary conditions and numerical settings

Based on Eqs. (3)-(5), the power-law velocity profile was applied to the inlet of the computational domain in this thesis. The reference wind speed (U_{ref}) at the reference height (z_{ref}) is equal to 4 m/s. The reference height is twice the height of the lower building (H_1) in the street canyons. In other words, the value of z_{ref} is 24 m. As we all know, the Standards Australia/Standards New Zealand, AS.NZS 1170.2 [34] provides the Terrain Category 2. Based on the Terrain Category 2, the value of the power law exponent (α) in Eq. (4) is equal to 0.2. The turbulence intensity at the height of z_{ref} is 10%. For Eq. (4), the empirical constant C_μ is equal to 0.085. As the character length, l is the height of the lower building. The boundary conditions applied to the outlet, lateral sides, domain top and building planes in Section 3 were also used here. So did the numerical settings adopted in Section 2.3.

$$U = U_{H_1}(\frac{z}{z_{H_1}})^{\alpha} \quad (4)$$

$$k = \frac{3}{2}(uI)^2 \quad (5)$$

$$\varepsilon = C_\mu k^{3/2}/l \quad (6)$$

2.5 Species transport modeling

Carbon monoxide (CO) was applied to represent the traffic emissions. As shown in **Fig. 1**, all cases investigated have a planar source of CO located at the ground in the target street canyon. According to the previous study [35], all the pollutant sources adopted exactly the same

constant CO release rate in this article. The time-averaged concentration of CO can be calculated by the governing equation shown below:

$$\frac{\partial(C\,u_j)}{\partial x_j} = -\frac{\partial}{\partial x_j}(D_m + D_t)\frac{\partial C}{\partial x_j} + S \quad (7)$$

where u_j and C are the time-averaged velocity component and the time-averaged concentration of CO (kg/m^3) respectively. D_m represents the molecular diffusivity of CO, while D_t ($D_t = \mu_t / Sc_t$) is the turbulent diffusivity of CO. As the turbulent Schmidt number, Sc_t is set to 0.7. Denoting the CO release rate, S is equal to 1.25×10^{-6} kg/m^3/s, which is set according to the pollutant emission rate for the real street located in urban areas with high traffic flux.

3. Results and discussion

3.1 Wind flow patterns in the target street canyons

In this section, we have mainly studied how the building layouts and envelope features affect the wind flow patterns within the street canyons of interest. The concept of velocity ratio was applied here, which means the ratio of the local velocity magnitude to the reference velocity magnitude (U_{ref} = 4 m/s).

3.1.1 Effects of building layouts on wind flow patterns

According to the simulation results shown in **Fig. 6**, it's obvious that building layouts play important roles in forming the wind environment in urban areas. On the whole, the velocity ratio in the symmetrical canyon is significantly higher than those in the asymmetrical canyons, while the step-down street canyon acquires the minimal wind velocity. For the symmetrical building layout, the wind flow in the target street canyon is dominated by an overarching clockwise recirculation. Contrary to this, one more recirculation will appear in the upper area when the step-up or step-down layout is adopted.

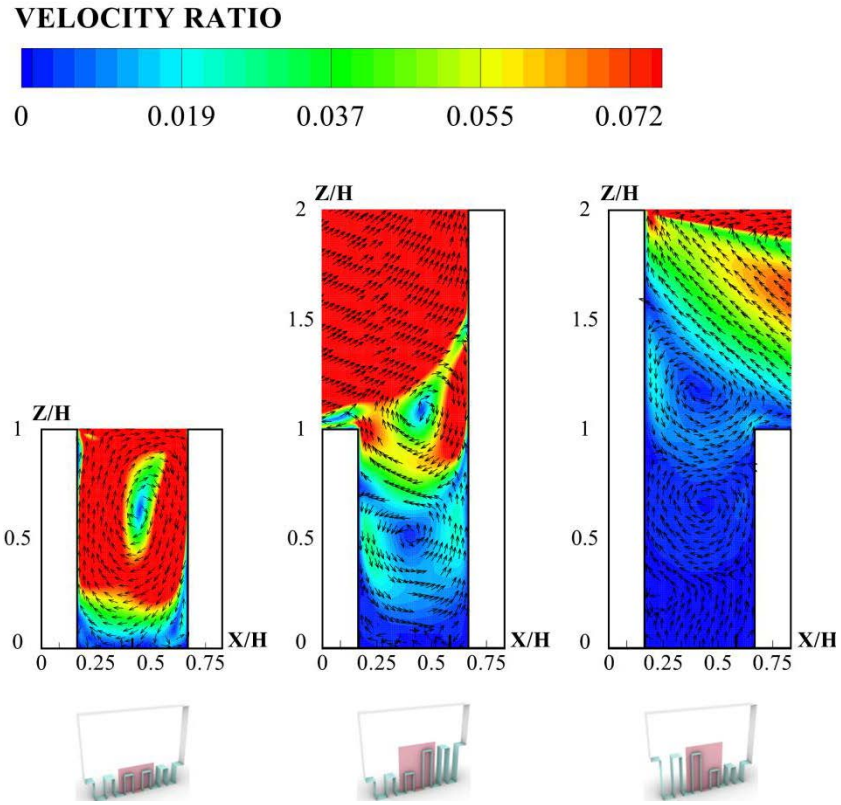

(a) (b) (c)

Fig. 6. Wind flow patterns for cases with flat facades: (a) Case NS; (b) Case Nu; and (c) Case Nd.

3.1.2 Effects of envelope features on wind flow patterns

Fig. 7 describes in detail how the wind flow patterns will change in the step-down canyon, when balconies, overhangs and wing walls replace the flat facade separately. Apparently, there are two major recirculation flows in the case without any envelope features (Case Nd), the upper one flowing counterclockwise and the lower one flowing clockwise. Meanwhile, there also exists an upward flow at the bottom of the canyon. However, in the case using balconies and the case adopting overhangs, the clockwise recirculation disappears. Instead, the wind flows inside these two canyons are dominated by the stronger upward flows and the centers of the counterclockwise flows move up slightly, compared to the case with flat facades. In the upper part of the street canyon, the airflow blows obliquely to the higher building when overhangs

are used, bringing a small recirculation to the fifth floor of the upstream building. For the case applying wing walls, two recirculation flows appear. But the lower clockwise flow is weaker than that in Case Nd and the center point of the counterclockwise recirculation moves down a little.

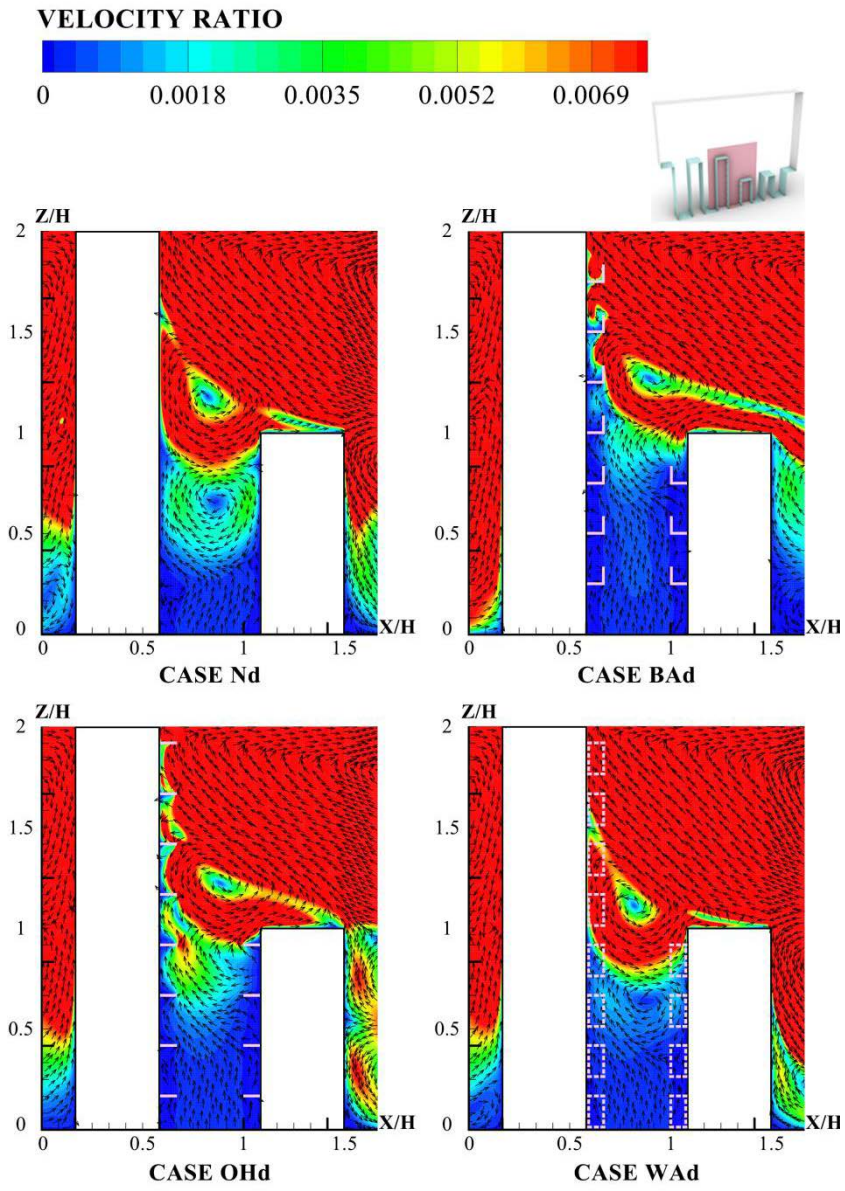

Fig. 7. Wind flow patterns for the step-down street canyon.

As for the step-up canyon with no envelope features, the upper recirculation is clockwise and the lower one is counterclockwise (see **Fig.8**), which is just the opposite of the situation in the

step-down canyon. And the clockwise recirculation has higher wind speeds than the counterclockwise one. Due to the presence of balconies and overhangs, the clockwise recirculation gets weaker and the lower recirculation in the canyon dissolves, replaced by the winding upward airflow. Meanwhile, the center of the upper clockwise flow shifts up slightly, which also moves a little toward the downstream building in the case using overhangs. In the areas around balconies, the wind patterns are disorderly. When overhangs are applied, a small recirculation flow appear at the fifth floor of the downstream building, which is in direct contradiction to the step-down case. Though with lower velocities, the wind flow pattern within the canyon using wing walls are nearly the same as that of the case without envelope features. This phenomenon can be attributed to the wing walls being parallel to the primary airflows inside the target canyon.

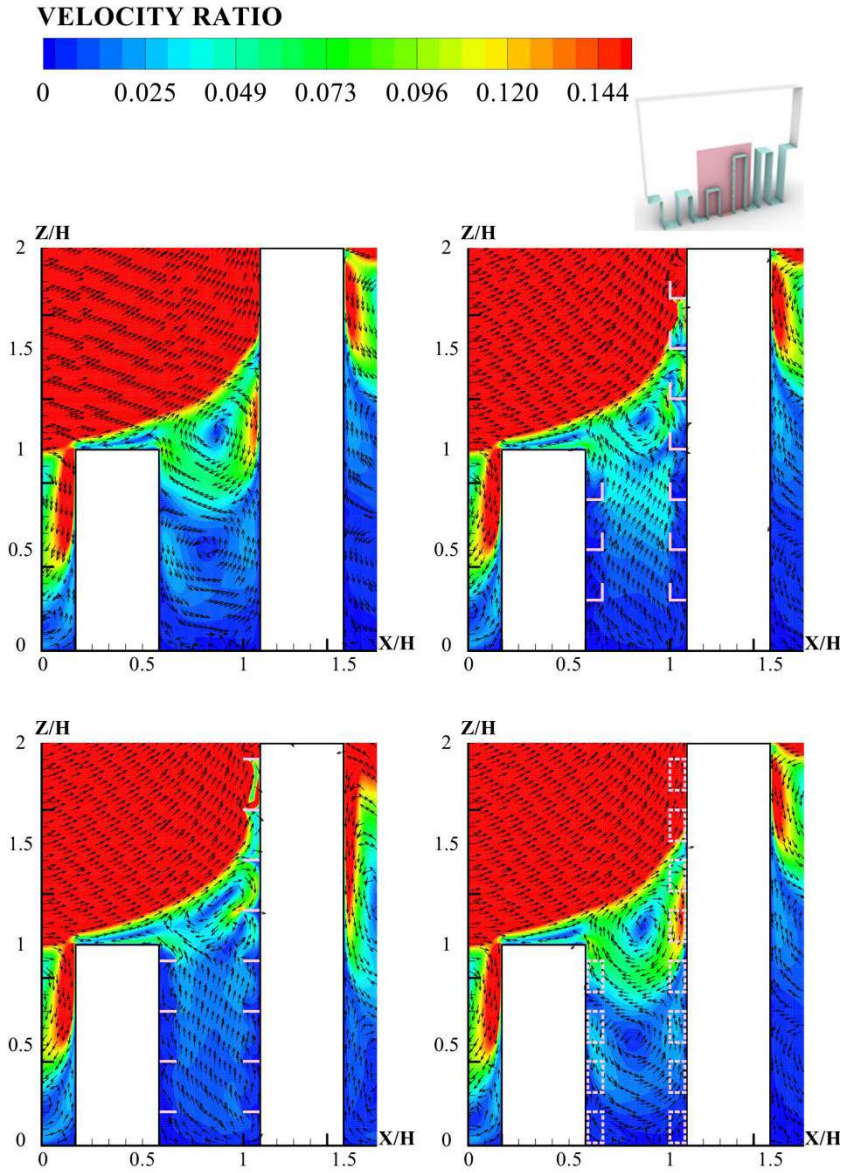

Fig. 8. Wind flow patterns for the step-up street canyon.

3.2 Pollutant dispersion in the target street canyons

This section discusses the effects that various building layouts and envelope features have on the pollutant transmissions inside urban street canyons. It's worth noting that we adopted a planar pollutant source located at the center of the canyon bottom. This section also defined the concept of concentration ratio which means the ratio of the local CO concentration (C) to the reference CO concentration at the planar source (C_0).

3.2.1 Effects of building layouts on pollutant dispersion

The simulation results illustrated by **Fig. 9** indicates evidently that building layouts have essential effects on the pollutant transmissions inside street canyons. Compared to the symmetric street canyon, the step-up and step-down layouts make the pollutant concentration ratio inside the target canyon increase significantly. In general, the step-down street canyon acquires the worst situation (the red zone with absolute value of 0.082 kg/m^3), followed by the step-up street canyon.

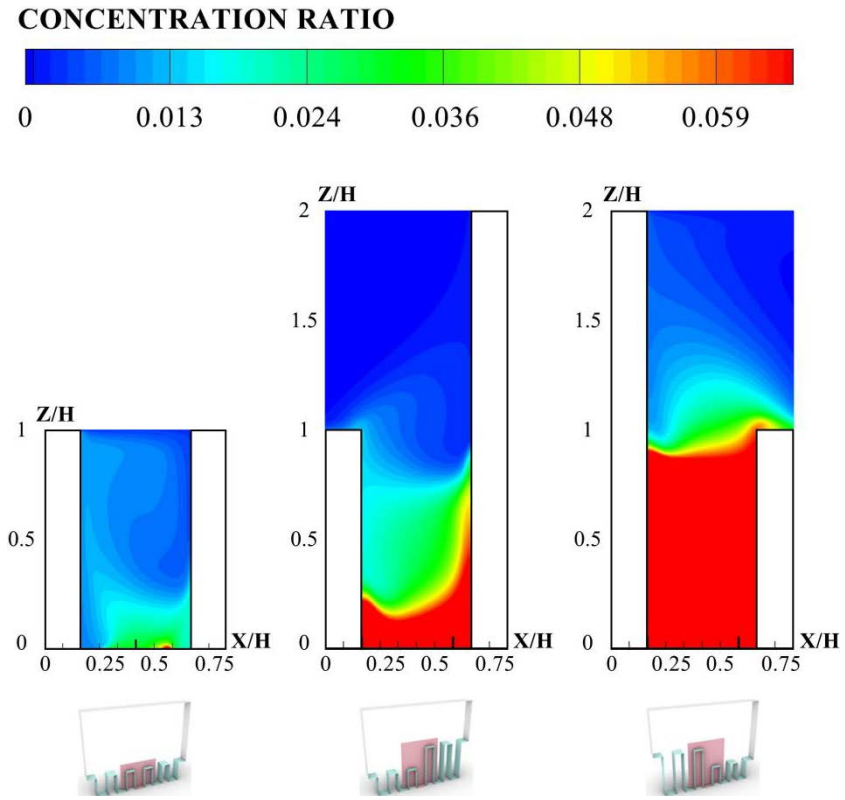

(a) (b) (c)

Fig. 9. Pollutant concentration ratio for cases with flat facades: (a) Case NS; (b) Case Nu; and (c) Case Nd.

3.2.2 Effects of envelope features on pollutant dispersion

Fig. 10 shows the pollutant concentration distributions within the step-down canyons with flat facades, balconies, overhangs and wing walls averagely. Obviously, all these three kinds of envelope features can lead to a significant increase in the pollutant concentration ratio, especially the balcony.

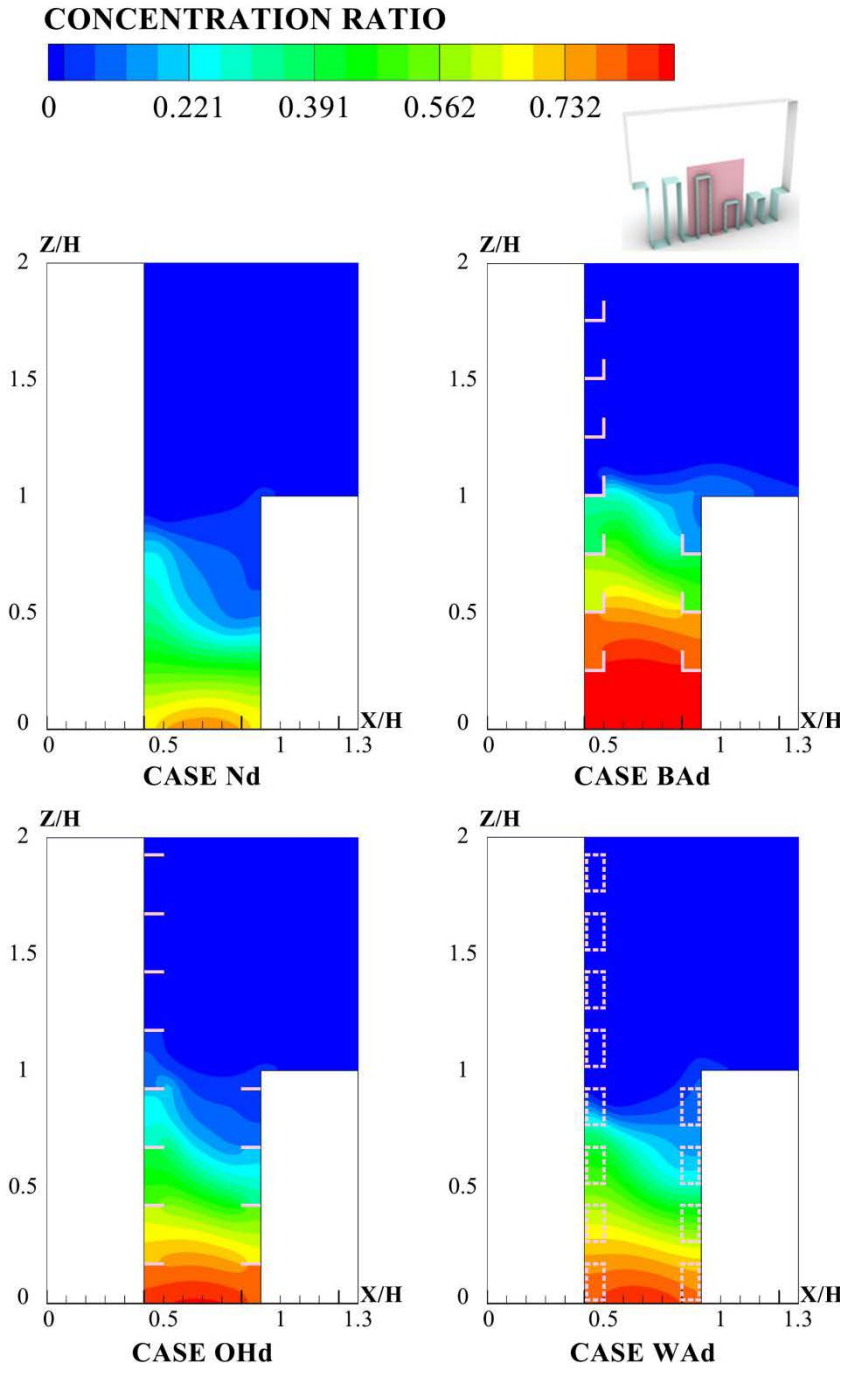

Fig. 10. Pollutant concentration for the step-down canyon.

Generally speaking, for the step-up canyon, the windward side of the downstream building has higher concentration ratios than the leeward side of the upstream building when there are no envelope features (see **Fig. 11**). This is because the counterclockwise airflow is weaker than the dominant clockwise flow, which can take the pollutant to the windward side first. The situation is similar when wing walls are used, now that those wing walls are set parallel to the primary airflow recirculation inside the canyon. However, the applications of balconies and overhangs will make the situation just the opposite, especially on the first and second floors. The upward airflow at the canyon bottom blowing obliquely to the upstream building's leeward side, which is blocked by the balconies and overhangs on lower floors, can account for this phenomenon. Overall, the pollutant concentration inside the canyon is highest when balconies are present. Nevertheless, compared to the case without envelope features, the concentration ratio in areas inside the balcony decreases on the fourth floor of the upstream building as well as the second, third and fourth floors of the downstream building when balconies are used.

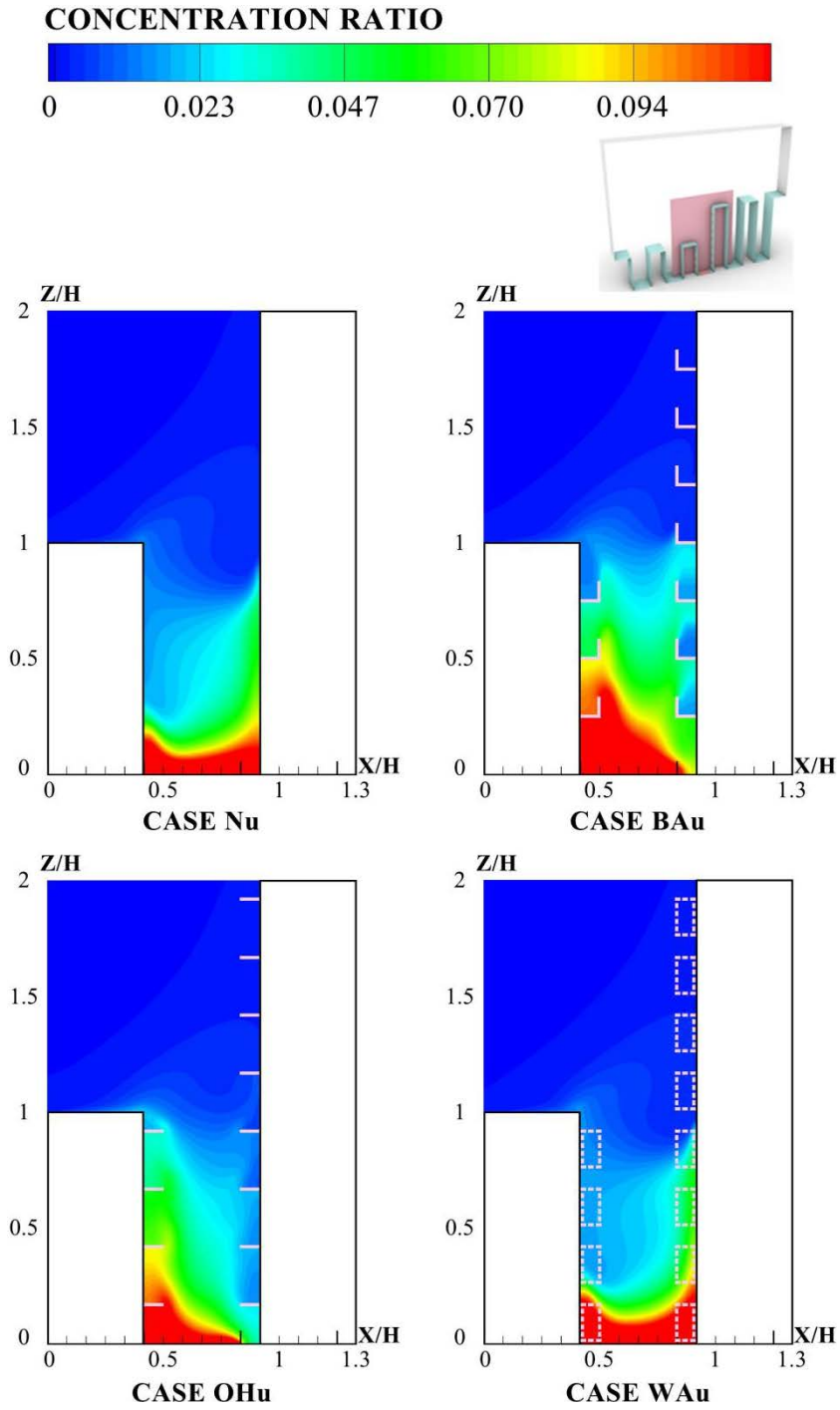

Fig. 11. Pollutant concentration for the step-up canyon.

3.3 Personal intake fraction (*P_IF*) in the street canyon

This section applies the non-dimensional definition of *P_IF* change ratio which means the growth ratio or the decline ratio of the *P_IF* values. **Fig. 12** and **Fig. 13** illustrate the *P_IF*

change ratios inside the set-down and the set-up canyons severally when different envelope features are present, compared to the canyon with the same building layout and flat facades. On the whole, among all the three kinds of envelope features, the wing walls have the least impact on the *P_IF* values, whether in set-down canyons or in set-up canyons.

Fig. 12 *P_IF* change ratio between the step-down canyon with flat facade and those with envelope features

Fig. 13 *P_IF* change ratio between the step-up canyon with flat facade and those with envelope features.

In general, for the step-down street canyon, the applications of envelope features always significantly increase the *P_IF* values at both the leeward side of the higher building and the windward side of the lower building. Only when wing walls or overhangs are used, will the reduction of the *P_IF* value appear on the upstream higher building's leeward side. In the

presence of wing walls, the decline ratio of *P_IF* values only occurs on the fifth floor. However, the *P_IF* value decreases on the sixth, seventh and eighth floor when overhangs are adopted. Additionally, among all those set-down cases, the fifth floor at the higher building's leeward side acquires the largest growth ratio of *P_IF*. Contrary to this, the sixth floor at the higher building's leeward side has the smallest growth ratio of *P_IF*. When it comes to the fist floor, which is closest floor to the pollutant source, it's appropriate to chose wing walls while the application of balconies should be avoided.

As for the step-up street canyons, the change ratios of *P_IF* due to the presence of envelope features are always less than 100% in most cases. Nevertheless, the growth ratios of *P_IF* on the second, third and fourth floors of the upstream lower building's leeward side are more than 150%, when overhangs are attached to the facades. Additionally, when balconies exist in the street canyon, the *P_IF* growth ratio is even as much as 314% on the second floor of the lower building's leeward side. Different from the set-down canyon, adopting overhangs is the best choice for both the leeward and the windward first floor in the step-up canyon.

3.4 Daily pollutant exposure in the canyon

In this section, the impacts of two building layouts and three envelope features on the daily pollutant exposure (E_d) were analyzed quantitively. The E_d values for the windows at the leeward side of the upstream building and the windward side of the downstream building are shown by **Table 4** and **Table 5**, respectively. Obviously, for all cases, the value of E_d will decrease with the distance between the window and the ground increasing gradually. Overall, among all those envelope features, the balcony can bring the most evident changes to the *Ed* values at both the leeward side and the windward side, followed by the overhang. Additionally, when balconies are used, the E_d value for the leeward side will increase compared to the situation with flat facades, whether in the step-up canyon or the step-down canyon. However,

there is an exception, namely the fourth floor in the step-up canyon. The introduction of overhangs can make the first, second and third floor of the upstream building obtain smaller E_d values than the flat facades. As for the windward side in the step-up canyon, the application of balconies or overhangs can make E_d values decrease evidently, except the fifth floor. Nevertheless, the introduction of wing walls will get higher exposure risks at the windward side in the step-up canyon, in spite of the sixth floor. Different from this, the exposure risks at the windward side in the step-down canyon will get growths, when balconies, overhangs or wing walls are used.

Table 4. Daily pollutant exposure (E_d) for leeward windows in different cases.

Cases	Windows	*Ed* (unit: kmol/m³/day)	
		Step-up street canyons	Step-down street canyons
Flat facade	L1	983.94	4360.04
	L2	164.58	2972.23
	L3	116.67	1968.36
	L4	100.21	995.02
	L5		71.03
	L6		57.28
	L7		48.52
	L8		42.22
Balcony	L1	1295.38	6210.29
	L2	682.00	5474.28
	L3	298.15	4270.12
	L4	91.27	2488.56
	L5		222.57
	L6		83.22
	L7		65.17
	L8		57.48
Overhang	L1	981.80	5494.82
	L2	591.32	4436.39
	L3	404.16	2904.93
	L4	254.46	1350.27
	L5		463.68
	L6		52.67
	L7		43.03
	L8		35.92
Wing walls	L1	940.89	5343.12
	L2	217.81	4415.30
	L3	111.05	3240.63
	L4	105.01	1221.28
	L5		66.38
	L6		57.64
	L7		50.82
	L8		44.83

Table 5. Daily pollutant exposure (E_d) for windward windows in different cases.

Cases	Windows	E_d (unit: kmol/m³/day)	
		Step-up street canyons	Step-down street canyons
Flat facade	W1	882.26	4379.96
	W2	513.50	2340.37
	W3	383.20	665.16
	W4	187.81	502.48
	W5	18.78	
	W6	16.36	
	W7	13.68	
	W8	11.06	
Balcony	W1	370.69	6190.58
	W2	125.74	5308.76
	W3	105.17	3729.45
	W4	134.84	841.00
	W5	24.67	
	W6	15.77	
	W7	11.49	
	W8	9.65	
Overhang	W1	137.14	5372.07
	W2	104.79	3882.45
	W3	104.33	1484.71
	W4	73.85	557.68
	W5	39.69	
	W6	15.86	
	W7	11.04	
	W8	7.42	
Wing walls	W1	1107.64	5132.75
	W2	619.13	3621.16
	W3	446.53	1504.63
	W4	320.92	825.77
	W5	19.23	
	W6	16.19	
	W7	13.90	
	W8	11.43	

4. Conclusion

In this paper, we have investigated how the step-down and step-up layouts can affect the wind flow patterns, pollutant transmission and pollutant exposure risks of pedestrians as well as near-road residents. On this basis, the influences of balcony, overhang and wing walls have also been assessed. The main findings are summarized as follows:

i. As for near wall regions, the airflow structure has a series of evident modifications when envelope features are introduced.

ii. Among the three different building configurations, the step-down canyon acquires largest pollutant concentration, followed by the step-up street canyon.

iii. In terms of the step-down street canyon, both the leeward side of the taller building and the windward side of the lower building suffer a lot from the increase of *P_IF*, when envelope features are adopted. The largest *P_IF* change ratio occurs to the fifth floor of the upstream building, when overhangs are applied to the step-down street canyon.

iv. Among the three commonly-used envelope features, wing walls affect the wind flow and pollutant transmission inside asymmetric canyons at the minimal degree. In contrast, the application of balconies generally brings the most obvious modifications.

5. Limitations and future research

This study has mainly focused on urban street canyons with asymmetric configurations, including the step-up canyon and the step-down canyon. Note that all the street canyons have an aspect ratio of 2. Further study considering with different aspect ratios are worthwhile being investigated in the future. According to the aforementioned results, we can draw such a conclusion that the combination of building layouts and envelope features plays an essential role in shaping wind flow patterns and affecting pollutant exposure inside street canyons. Although the simulation models used in this paper resulted in reasonable findings, other

numerical settings including unsteady-state turbulence modelling approaches as well as modeling constants are still waiting for further investigations. At the same time, more efforts are required to fully understand the impacts of turbulent kinetic energy, convective and turbulent mass flux on the simulation accuracy. Additionally, in order to explore the actual situation of pollutant dispersion in urban street canyons, we have already conducted a series of scaled outdoor experiments. On the whole, these outdoor experiments involve street canyons with different orientations, different aspect ratios, and different facade components. In the future, outdoor measurement data obtained from these scaled experiments will be analysed and compared with the simulated data. So that we can further verify the hypothesis put forward in this article.

Acknowledgement

The work described in this paper was supported by National Natural Science Foundation of China (grant no 51808342) and Natural Science Foundation of Shenzhen (JCYJ20180305125219726).

References

[1] C. Lu, L. Cao, D. Norbäck, Y. Li, J. Chen, Q. Deng, Combined effects of traffic air pollution and home environmental factors on preterm birth in China. Ecotoxicol. Environ. Saf. 184 (2019) 109639.

[2] M. Hachem, N. Saleh, A.-C. Paunescu, I. Momas, L. Bensefa-Colas, Exposure to traffic air pollutants in taxicabs and acute adverse respiratory effects: a systematic review. Sci Total Environ. 693 (2019) 133439.

[3] W. Ji, B. Zhao, Estimating mortality derived from indoor exposure to particles of outdoor origin, PloS One 10 (4) (2015) 15.

[4] J. Hang, Z. Xian, D. Wang, C.M. Mak, B. Wang, Y. Fan, The impacts of viaduct settings and street aspect ratios on personal intake fraction in three-dimensional urban-like geometries, Build. Environ. Times 143 (2018) 138-162.

[5] R. Buccolieri, M. Sandberg, S. Di Sabatino, City breathability and its link to pollutant concentration distribution within urban-like geometries, Atmos. Environ. 44 (15) (2010) 1894-1903.

[6] Y. Du, C.M. Mak, Z. Ai, Modelling of pedestrian level wind environment on a high-quality mesh: a case study for the HKPolyU campus, Environ. Model. Software 103 (2018) 105-119.

[7] Y. Du, C.M. Mak, Y. Li, Application of a multi-variable optimization method to determine lift-up design for optimum wind comfort, Build. Environ. 131 (2018) 242-254.

[8] Y. Du, C.M. Mak, Y. Li, A multi-stage optimization of pedestrian level wind environment and thermal comfort with lift-up design in ideal urban canyons, Sustain. Cities Soc. 46 (2019) 101424.

[9] D. Cui, G. Hu, Z. Ai, Y. Du, C.M. Mak, K. Kwok, Particle image velocimetry measurement and CFD simulation of pedestrian level wind environment around U-type street canyon, Build. Environ. Times 154 (2019) 239-251.

[10] C. Gromke, B. Ruck, Pollutant concentrations in street canyons of different aspect ratio with avenues of trees for various wind directions, Bound.-Layer Meteorol. 144 (1) (2012) 41-64.

[11] Y. Du, B. Blocken, S. Pirker, A novel approach to simulate pollutant dispersion in the built environment: transport-based recurrence CFD, Build. Environ. 170 (2020) 106604.

[12] J. Rodríguez-Algeciras, A. Tablada, A. Matzarakis, Effect of asymmetrical street canyons on pedestrian thermal comfort in warm-humid climate of Cuba, Theor. Appl Climatol. 133 (2018) 663-679.

[13] Z. Li, H. Zhang, C.-Y. Wen, A.-S. Yang, Y.-H. Juan, Effects of height-asymmetric street canyon configurations on outdoor air temperature and air quality, Build. Environ. 183 (2020) 107195.

[14] S.-J. Park, J.-J. Kim, W. Choi, E.-R. Kim, C.-K. Song, E. Pardyjak, Flow characteristics around step-up street canyons with various building aspect ratios, Bound.-Layer Meteorol. 174 (2020) 411-431.

[15] P. Nejat, F. Jomehzadeh, H.M. Hussen, J.K. Calautit, A. Majid, M. Zaimi, Application of wind as a renewable energy source for passive cooling through windcatchers integrated with wing walls, Energies 11 (10) (2018) 2536.

[16] Z. Ai, C.M. Mak, Wind-induced single-sided natural ventilation in buildings near a long street canyon: CFD evaluation of street configuration and envelope design, J. Wind Eng. Ind. Aerod. 172 (2018) 96-106.

[17] F. Ghadikolaei, D. Ossen, M. Mohamed, Effects of wing wall at the balcony on the natural ventilation performance in medium-rise residential buildings, J. Build. Eng. 31 (2020) 101316.

[18] L. He, J. Hang, X. Wang, B. Lin, X. Li, G. Lan, Numerical investigations of flow and passive pollutant exposure in high-rise deep street canyons with various street aspect ratios and viaduct settings, Sci. Total Environ. 584 (2017) 189-206.

[19] B. Blocken, R. Vervoort, T. van Hooff, Reduction of outdoor particulate matter concentrations by local removal in semi-enclosed parking garages: a preliminary case study for Eindhoven city center, J. Wind Eng. Ind. Aerod. 159 (2016) 80-98.

[20] C.-H. Liu, C.-T. Ng, C.C. Wong, A theory of ventilation estimate over hypothetical urban areas, J. Hazard Mater. 296 (2015) 9-16.

[21] X. Xie, C.-H. Liu, D.Y. Leung, Impact of building facades and ground heating on wind flow and pollutant transport in street canyons, Atmos. Environ. Times 41 (39) (2007) 9030-9049.

[22] W.H. Snyder, Guideline for Fluid Modeling of Atmospheric Diffusion. Fluid Modeling Report No. 10, US EPA, Research Triangle Park, NC, 1981.

[23] G. Habilomatis, A. Chaloulakou, A CFD modeling study in an urban street canyon for ultrafine particles and population exposure: the intake fraction approach, Sci. Total Environ. 530 (2015) 227-232.

[24] J. Hang, Z.W. Luo, X.M. Wang, L.J. He, B.M. Wang, W. Zhu, The influence of street layouts and viaduct settings on daily carbon monoxide exposure and intake fraction in idealized urban canyons, Environ. Pollut. 220 (2017) 72-86.

[25] Z. Luo, Y. Li, W.W. Nazaroff, Intake fraction of nonreactive motor vehicle exhaust in Hong Kong, Atmos. Environ. 44 (15) (2010) 1913-1918.

[26] C. Chau, E. Tu, D. Chan, J. Burnett, Estimating the total exposure to air pollutants for different population age groups in Hong Kong, Environ. Int. 27 (8) (2002) 617-630.

[27] X.-X. Li, D.Y. Leung, C.-H. Liu, K.M. Lam, Physical modeling of flow field inside urban street canyons, J.Appl. Meteorol. Clim. 47 (7) (2008) 2058-2067.

[28] Effects of envelope features on wind flow and pollutant exposure in street canyons

[29] CFD simulation of flow in a long street canyon under a perpendicular wind direction: Evaluation of three computational settings

[30] J. Franke, A. Hellsten, K.H. Schlunzen, B. Carissimo, The COST 732 Best Practice Guideline for CFD simulation of flows in the urban environment: a summary, Int. J. Environ. Pollut. 44 (1-4) (2011) 419-427.

[31] Y. Tominaga, A. Mochida, R. Yoshie, H. Kataoka, T. Nozu, M. Yoshikawa, T. Shirasawa, AIJ guidelines for practical applications of CFD to pedestrian wind environment around buildings, J. Wind Eng. Ind. Aerod. 96 (10-11) (2008) 1749-1761.

[32] Y. Tominaga, T. Stathopoulos, Numerical simulation of dispersion around an isolated cubic building: comparison of various types of k-ϵ models, Atmos. Environ. 43 (20) (2009) 3200-3210.

[33] W.-W. Li, R.N. Meroney, Gas dispersion near a cubical model building. Part I. Mean concentration measurements, J. Wind Eng. Ind. Aerod. 12 (1) (1983) 15-33.

[34] AS. Nzs 1170.2, Australian/New Zealand Standard, Structural Design Action Parts 2: Wind Actions, Standards Australia & Standards New Zealand, Sydney, 2002.

[35] K. Zhang, G. Chen, X. Wang, S. Liu, C.M. Mak, Y. Fan, J. Hang, Numerical evaluations of urban design technique to reduce vehicular personal intake fraction in deep street canyons, Sci. Total Environ. 653 (2019) 968–994.